

# Journal of Biomedical Optics

BiomedicalOptics.SPIEDigitalLibrary.org

## **Surface modification of alignment layer by ultraviolet irradiation to dramatically improve the detection limit of liquid-crystal-based immunoassay for the cancer biomarker CA125**

Hui-Wen Su  
Mon-Juan Lee  
Wei Lee

# Surface modification of alignment layer by ultraviolet irradiation to dramatically improve the detection limit of liquid-crystal-based immunoassay for the cancer biomarker CA125

Hui-Wen Su,<sup>a</sup> Mon-Juan Lee,<sup>b,\*</sup> and Wei Lee<sup>a,\*</sup>

<sup>a</sup>National Chiao Tung University, Institute of Imaging and Biomedical Photonics, College of Photonics, Guiren District, Tainan 71150, Taiwan

<sup>b</sup>Chang Jung Christian University, Department of Bioscience Technology, Guiren District, Tainan 71101, Taiwan

**Abstract.** Liquid crystal (LC)-based biosensing has attracted much attention in recent years. We focus on improving the detection limit of LC-based immunoassay techniques by surface modification of the surfactant alignment layer consisting of dimethyloctadecyl[3-(trimethoxysilyl)propyl]ammonium chloride (DMOAP). The cancer biomarker CA125 was detected with an array of anti-CA125 antibodies immobilized on the ultraviolet (UV)-modified DMOAP monolayer. Compared with a pristine counterpart, UV irradiation enhanced the binding affinity of the CA125 antibody and reproducibility of immunodetection in which a detection limit of 0.01 ng/ml for the cancer biomarker CA125 was achieved. Additionally, the optical texture observed under a crossed polarized microscope was correlated with the analyte concentration. In a proof-of-concept experiment using CA125-spiked human serum as the analyte, specific binding between the CA125 antigen and the anti-CA125 antibody resulted in a distinct and concentration-dependent optical response despite the high background caused by nonspecific binding of other biomolecules in the human serum. Results from this study indicate that UV modification of the alignment layer, as well as detection with LCs of large birefringence, contributes to the enhanced performance of the label-free LC-based immunodetection, which may be considered a promising alternative to conventional label-based methods. © 2015 Society of Photo-Optical Instrumentation Engineers (SPIE) [DOI: [10.1117/JBO.20.5.057004](https://doi.org/10.1117/JBO.20.5.057004)]

Keywords: liquid-crystal-based immunodetection; cancer biomarker; CA125; label-free immunodetection.

Paper 150068PRR received Feb. 4, 2015; accepted for publication May 4, 2015; published online May 22, 2015.

## 1 Introduction

Immunodetection of cancer biomarkers is an essential procedure in cancer detection and diagnosis. Cancer biomarkers, or tumor antigens, are specific proteins or molecules secreted by cancer cells. An elevated concentration of cancer biomarkers in blood or urine implicates a higher risk for cancer and is considered a useful indication for assessing cancer progression and a patient's response to cancer treatment. Current clinical practices in cancer screening utilize immunoassay methods such as the sandwich assay, which depends on the specific binding of the biomarker by two types of primary antibodies that recognize different epitopes. Detection is achieved by labeling one of the primary antibodies with chemiluminescence or by reacting the immunocomplex with a labeled secondary antibody. The amount of chemiluminescence released by labeled molecules is then quantitated to determine the level of cancer biomarkers.

Due to the complicated and time-consuming assay procedure, new techniques have been developed to more efficiently and sensitively detect the immunocomplexes. These include electrochemical and optical immunosensors, protein chips, and nanomaterial-based immunoassays.<sup>1,2</sup> However, except

for several electrochemical methods and optical sensing approaches such as surface plasmon resonance, most of the immunodetection approaches are label-based. The requirement of various labeled antibodies, as well as the labeling reaction, increases the cost of the immunoassay, not to mention the expensive equipment for immunofluorescence detection. Therefore, development of label-free immunodetection techniques, in which only one type of primary antibody is necessary, is expected to reduce the cost of immunoassays and to simplify cancer screening procedures.

CA125 is a mucin-like glycoprotein with a molecular weight greater than 200 kDa. It was first detected over 30 years ago using the OC125 monoclonal antibody, which provides the basis for immunoassays to detect and monitor the progression of epithelial ovarian cancer.<sup>3</sup> Later studies suggest that CA125 is also observed in other malignancies such as breast and gastric cancers.<sup>4,5</sup> Conventional CA125 immunoassay has a detection limit of 15 U/mL, which is sufficient to detect the threshold level of 35 U/ml CA125 that correlates with the diseased state.<sup>6</sup> Nevertheless, various innovative immunodetection technologies for the detection of CA125 have been reported, such as arrayed microsensor chips,<sup>6</sup> a bead-based enzyme-linked immunosorbent assay (ELISA),<sup>7</sup> a fluorescence immunoassay

\*Address all correspondence to: Mon-Juan Lee, E-mail: [mjlee@mail.cjcu.edu.tw](mailto:mjlee@mail.cjcu.edu.tw); or Wei Lee, E-mail: [wlee@nctu.edu.tw](mailto:wlee@nctu.edu.tw)

employing the ALYGNSA antibody-orientation system,<sup>8</sup> electrochemical biosensors,<sup>9–12</sup> and nanomaterial-based colorimetric immunoassays.<sup>13</sup> These approaches aim at further lowering the detection limit and sample volume, providing alternatives to multiplex and high-throughput screening of cancer biomarkers.

Since Abbott's group reported the use of 4-cyano-4'-pentylbiphenyl (5CB)—a liquid crystal (LC)—as a sensing element to detect biomolecules, LC-based biosensors have received much attention.<sup>14–18</sup> The birefringent properties of the anisotropic mesogenic molecules are exploited in LC-based biosensing, in which the presence of biomolecules, as well as their binding and reaction with other molecules, disturbs the orientation of LCs and triggers a change in their optical appearance.<sup>19,20</sup> Currently, LC-based biosensing techniques are developed for the signal amplification of protein–peptide, protein–protein, and protein–receptor binding,<sup>15,21–23</sup> real-time monitoring of enzymatic reactions,<sup>24,25</sup> recognition of the orientation of immobilized proteins,<sup>17,18</sup> immunodetection of the specific binding between antigens and antibodies,<sup>20,26–29</sup> glucose biosensing,<sup>30</sup> and DNA hybridization assays.<sup>31–33</sup> Although the development of LC-based immunodetection is still at its early stage and its sensitivity has not reached a satisfying level for clinical application, several attempts have been made to study the correlation between detection sensitivity and the molecular weight of the immunocomplex.<sup>26</sup> In addition, a strategy to quantitate antibody concentration is proposed in a LC-based microfluidic immunoassay.<sup>29</sup>

In LC-based immunodetection, proteins or antibodies are immobilized on a glass substrate coated with an alignment layer consisting of silane surfactants such as dimethyloctadecyl[3-(trimethoxysilyl)propyl]ammonium chloride (DMOAP).<sup>20,26,34</sup> Although proteins and antibodies tend to adsorb on the DMOAP monolayer, subsequent washing procedures to eliminate nonspecific binding may result in gradual dissociation of the immobilized antigen, antibody or immunocomplex, reducing the sensitivity and reproducibility of the immunoassay. In order to enhance the binding affinity of the LC aligning agent, modification of

DMOAP with ultraviolet (UV) light is expected to provide functional groups that enhance binding between the alignment layer and biomolecules.<sup>35,36</sup> Exposure to UV irradiation results in degradation of the alkylsiloxane self-assembled monolayer, and functional groups such as  $-\text{COOH}$ ,  $-\text{CHO}$ , and  $-\text{OH}$  are generated on the UV-irradiated surface, which tends to become more hydrophilic.<sup>37–40</sup> Oxygen produced via UV-induced ozonolysis is critical in the formation of these oxidized functional groups, which react with biomolecules and cells to facilitate the formation of hydrogen bonds and covalent bonds.<sup>38,41–43</sup>

In this study, a label-free and LC-based immunoassay with improved detection limit for the cancer biomarker CA125 was established by exploiting UV-modified DMOAP as the alignment layer and a eutectic nematic mixture exhibiting a large anisotropy in refractive index ( $\Delta n = 0.333$  at 589.3 nm and 20°C) as the LC sensing element. It is suggested that by increasing the binding affinity between the anti-CA125 antibody and DMOAP through UV modification, antibodies and immunocomplexes are stably attached to the alignment layer, thus triggering a more significant transition in the optical texture of LCs. In addition, a eutectic mixture of higher birefringence and wider nematic range, compared with the single-compound LC 5CB commonly used in other LC biosensing studies, is believed to respond more sensitively and reproducibly to the binding events of antigens and antibodies, giving rise to a lower detection limit compared to label-based fluorescence immunoassay.<sup>34,44</sup> Both strategies combined are expected to improve the accuracy, reproducibility and detection limit of LC-based immunodetection, as well as its potential in clinical application.

## 2 Materials and Methods

### 2.1 Materials

LCD-grade glass slides (15 mm × 20 mm) were purchased from Mesostate (Taiwan). DMOAP as the aligning agent was purchased from Sigma–Aldrich. The high- $\Delta n$  and multicomponent LC was obtained from Jiangsu Hecheng Display Technology

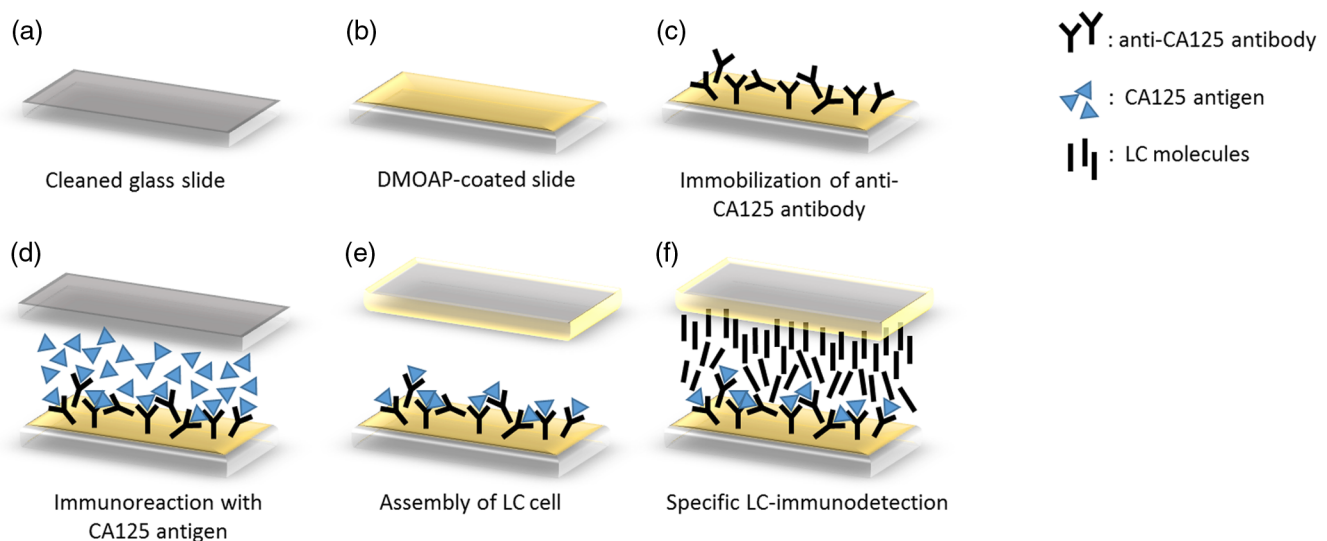


**Fig. 1** Sample preparation procedure of liquid crystal (LC)-based immunodetection: (a) Cleaning the glass slides; (b) coating with dimethyloctadecyl[3-(trimethoxysilyl)propyl]ammonium chloride (DMOAP) alignment layer; (c) immobilization of 0.01  $\mu\text{g}/\text{ml}$  anti-CA125 mouse antibody; (d) immunoreaction with the CA125 antigen; (e) assembly of the LC cell; (f) disruption of LC orientation by CA125 antigen–antibody immunocomplexes.

Co., Ltd. (HCCH, China). The UV lamp, the source of UV irradiation, was manufactured by DAJIUN. Recombinant human CA125 (MUC16) was purchased from R&D Systems. Monoclonal mouse anti-human CA125 antibodies were manufactured by Santa Cruz Biotechnology. All aqueous solutions were prepared using deionized (DI) water, which was purified by an RDI reverse osmosis/deionizer system.

## 2.2 Preparation of DMOAP-Coated Glass Slides

The procedure of sample preparation for LC-based immunoassay was depicted in Fig. 1. Glass slides were cleaned by immersing successively in an aqueous solution of detergent, DI water and 99% ethanol, with each step accompanied by ultrasonication for 15 min at room temperature (RT). The glass slides were dried under a stream of nitrogen and then baked at 74°C for 15 min. Subsequently, the cleaned glass slides were immersed in an aqueous solution containing 1% (v/v) DMOAP for 15 min at RT. Excess DMOAP was removed via ultrasonication in DI water for 1 min, followed by drying under a stream of nitrogen and heating at 100°C for 15 min. To prepare the UV-modified DMOAP alignment layer, the DMOAP-coated glass slide was exposed to broad-band UV light at 15 mW/cm<sup>2</sup> for 0–20 min (Fig. 2).

## 2.3 Immunoreaction

Prior to use, anti-CA125 mouse antibody and CA125 antigen of a desired concentration were prepared with DI water. The anti-CA125 antibody was immobilized on a DMOAP-coated glass substrate with or without UV modification in an array format. Each antibody array included at least nine replicates of anti-CA125 antibodies arranged in a 3 × 3 format at 0.01 μg/ml and 1 μl/spot. The antibody array was allowed to dry overnight at RT. Afterward, 10 μl of CA125 at the designated concentration was layered on the antibody array with a clean cover glass and reacted with anti-CA125 antibodies for 1 h at RT. The cover glass was then removed and the glass substrate was rinsed once

by tilting the glass slide and allowing 5-ml DI water to flow continuously through the DMOAP-coated surface to eliminate unbound antigen, followed by drying at RT.

To demonstrate the potential of LC-based immunodetection in analyzing clinical samples, a similar procedure in which the CA125 antigen was substituted with human serum (Valley Biomedical) spiked with 0, 0.01, 0.1, 1, 10, or 100 ng/ml CA125 was performed. To assess the specificity of LC-based immunodetection, antibodies against spermidine/spermine N<sup>1</sup>-acetyl transferase (SSAT) and β-catenin, both manufactured by Santa Cruz Biotechnology, were immobilized on UV-modified DMOAP at 0.01 μg/ml and 1 μl per spot, followed by reaction with 0, 0.1, or 1 μg/ml CA125.

## 2.4 Assembling the Liquid Crystal Cell

Spacers of 5.1 μm in size were dispensed on the four corners of a DMOAP-coated glass slide bearing the anti-CA125 antibody array and CA125 antigen–antibody immunocomplexes. After drying at RT for 2 h, an LC optical cell was constructed by covering the glass slide with another DMOAP-coated slide and sealed with epoxy glue. After another 2 h at RT, the LC was introduced into the cell by capillary action. The optical texture of the LC was observed under a crossed polarized microscope (OLYMPUS BX51) in the transmission mode.

## 2.5 Contact Angle Measurement

The contact angle of a 5 μl water droplet on DMOAP-coated glass substrates with or without UV modification was determined by an FTÅ200 instrument. All experiments were performed at a constant relative humidity of 50% at RT.

## 2.6 Fourier Transform Infrared Spectroscopy

Fourier transform infrared (FT-IR) spectra of intact and UV-modified DMOAP were obtained with a Nicolet iS10 FT-IR spectrometer in the transmission mode and 3M disposable IR

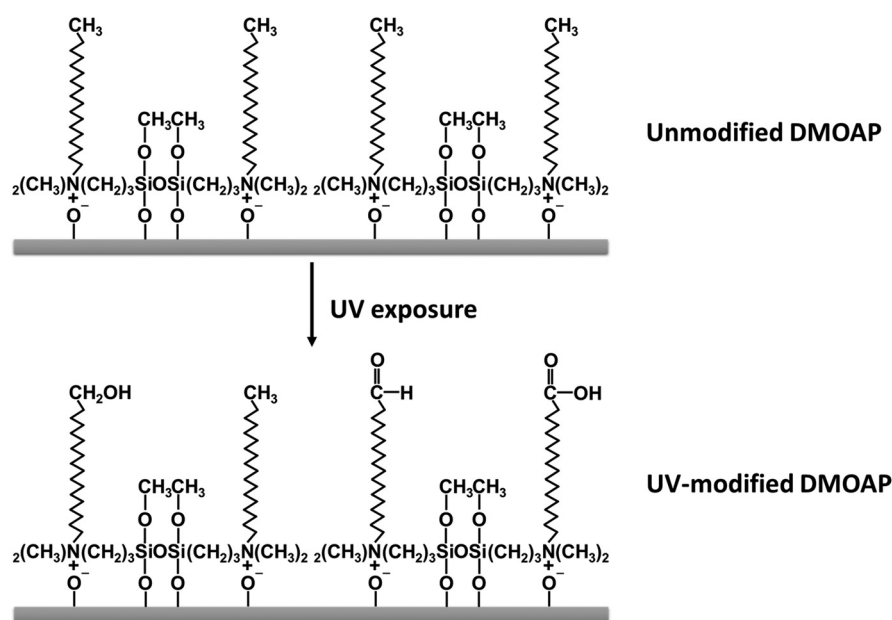


**Fig. 2** Surface modification of DMOAP alignment layer by ultraviolet (UV) irradiation. The glass slides were coated with DMOAP followed by UV exposure as described in Sec. 3.

cards (Type 61). A DMOAP solution of 1% (v/v) in methanol was dispensed on the IR cards, and then heated on a hot plate at 60°C for 1 h in order to remove residual methanol. After exposure to UV irradiation for 0, 1, or 5 min, IR spectra of DMOAP films were acquired with 32 scans and a 0.964  $\text{cm}^{-1}$  resolution in the range of 4000 – 800  $\text{cm}^{-1}$ . The FT-IR spectrum of a cleaned IR card was used as the background for all measurements, which remained unchanged after heating at 60°C for 1 h and exposed to UV irradiation at 15  $\text{mW}/\text{cm}^2$  for 1 min.

### 3 Results

#### 3.1 Characterization of Ultraviolet-Modified DMOAP Alignment Layer

##### 3.1.1 Contact angle measurement

In order to study the correlation between the UV exposure time and surface hydrophilicity, DMOAP alignment layers were irradiated with UV for 0–20 min, after which the contact angle of water was determined. As shown in Fig. 3, the intact DMOAP monolayer was slightly hydrophilic, with a water contact angle  $\theta$  of 87 deg. The contact angle of the UV-modified DMOAP alignment layer decreased with increasing UV exposure time, suggesting that the hydrophilicity of the surface was promoted. UV modification is thus considered a simple and effective approach to generating hydrophilic functional groups on alkyl-siloxane films such as DMOAP. Noticeably, because protein adsorption does not occur on hydrophilic surfaces with  $\theta < 65$  deg,<sup>45</sup> UV exposure in this study was limited to 1 min to provide sufficiently oxidized functional groups to bind the anti-CA125 antibody without significantly altering surface hydrophilicity.

##### 3.1.2 Fourier transform infrared spectroscopy

The types of functional groups or chemical bonds produced during UV irradiation were identified by subjecting samples of DMOAP with or without UV irradiation to FT-IR spectroscopic analysis (Fig. 4). The characteristic peak at 2850 – 3000  $\text{cm}^{-1}$  was contributed by the C–H stretching of alkane, which represents the alkyl chain of DMOAP. The

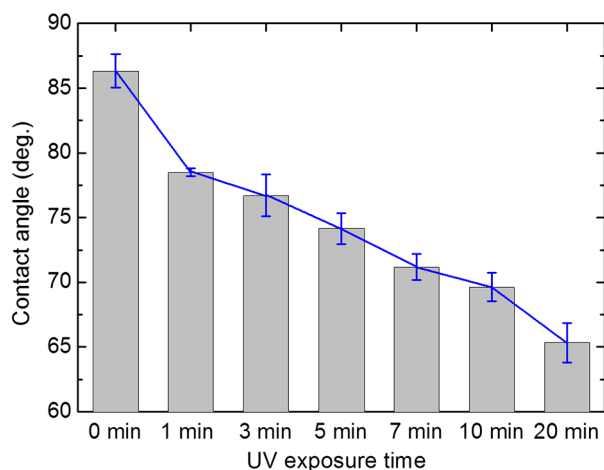


**Fig. 3** Correlation between the UV exposure time and water contact angle of DMOAP alignment layer. The DMOAP alignment layer was irradiated with UV for 0–20 min prior to contact angle measurement using an FTÅ200 instrument.

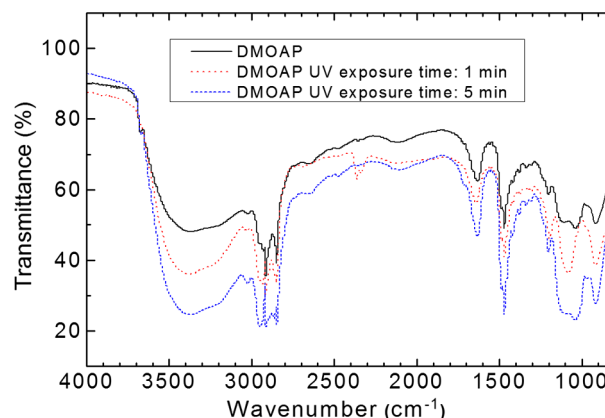


**Fig. 4** Fourier Transform Infrared (FT-IR) spectra of intact and UV-modified DMOAP films. The FT-IR spectra were obtained with a Nicolet iS10 FT-IR spectrometer in the transmission mode and 3M disposable IR cards (Type 61) as described in Sec. 2.

band at 3200 – 3500  $\text{cm}^{-1}$ , assigned to the O–H bond of the hydroxyl group, and that at 1100 – 1200  $\text{cm}^{-1}$ , resulting from C–O stretching of alcohols or aldehydes, increased in intensity with increasing UV exposure time, suggesting that the enhancement in hydrophilicity of DMOAP (Fig. 3) is attributed to the presence of more oxidized and polar functional groups. Furthermore, the intensity of peaks representing carbonyl groups (C=O) at 1600 – 1700  $\text{cm}^{-1}$  increased only when DMOAP was exposed to UV for 5 min (Fig. 4). These results suggest that a short UV exposure (1 min) of DMOAP as preferred in this study may give rise to hydroxyl groups instead of aldehyde or carboxylic acid groups.

#### 3.2 Liquid Crystal-Based Immunodetection with Ultraviolet-Modified DMOAP Alignment Layer

Anti-CA125 antibodies of 0.01  $\mu\text{g}/\text{ml}$  and 1  $\mu\text{l}$  per spot were immobilized on intact or UV-modified DMOAP alignment layer and reacted with various concentrations of the CA125 antigen for 1 h at RT, followed by detection with LC under a crossed polarized microscope. In the absence of antibodies or proteins, the nematic LC was aligned perpendicularly to the glass surface by the DMOAP monolayer and its optical texture was completely dark. The immobilized anti-CA125 antibodies alone were insufficient to disrupt the homeotropic alignment of LCs, and the optical appearance of LCs remained dark [Figs. 5(a) and 6(a)]. As the CA125 concentration was gradually increased, so was the number of antigen–antibody immunocomplexes, which resulted in significant disruption of the alignment of LCs because of their larger size. The optical texture of LCs, therefore, changed from dark to bright to reflect the amount of immunocomplexes present. In Fig. 5, the difference between the optical signals for each CA125 concentration was indiscernible because the concentration of the immobilized anti-CA125 antibody was suboptimal and was insufficient to form enough CA125 immunocomplexes to incur significant disruption of the LC alignment. On the other hand, UV modification of DMOAP gave rise to an alignment layer with a greater affinity toward anti-CA125 antibodies. Consequently, the loss of the immobilized antibody and CA125 immunocomplex during the washing procedure was drastically reduced, resulting in a better resolution of the

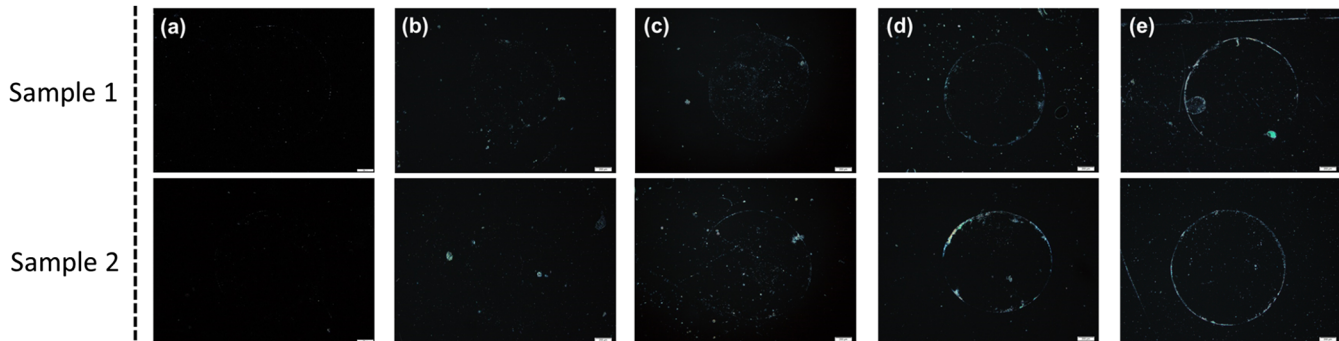


**Fig. 5** LC optical textures of the CA125 immunocomplex on an unmodified DMOAP alignment layer. Unmodified DMOAP monolayer was immobilized with an array of 0.01- $\mu\text{g/ml}$  anti-CA125 antibody and complexed with (a) 0-, (b) 0.01-, (c) 0.1-, (d) 1-, and (e) 10- $\mu\text{g/ml}$  CA125 antigen. The optical texture of the CA125 immunocomplex was determined by an OLYMPUS BX51 crossed polarized microscope in the transmission mode. Bar, 200  $\mu\text{m}$ .

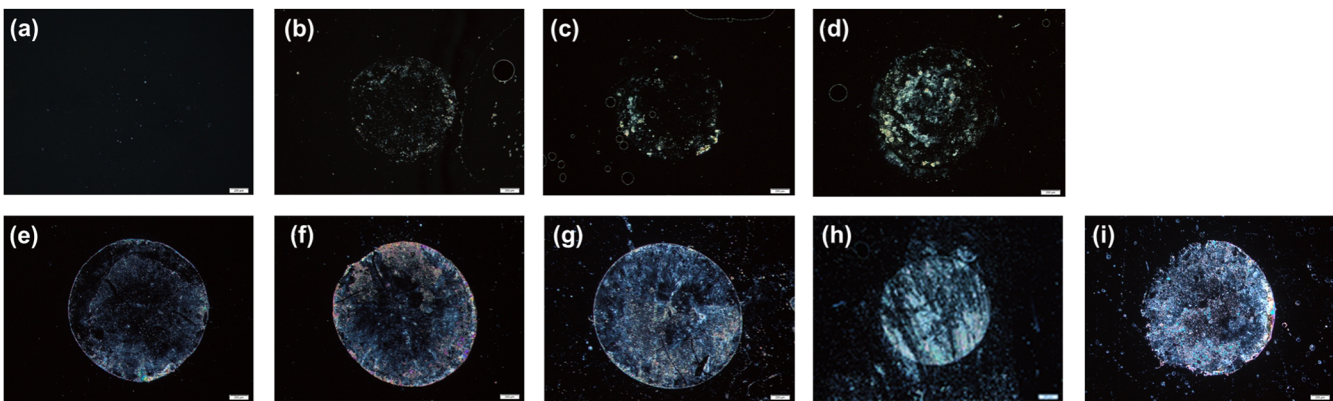


**Fig. 6** LC optical textures of the CA125 immunocomplex on a UV-modified DMOAP alignment layer. UV-modified DMOAP monolayer was immobilized with an array of 0.01- $\mu\text{g/ml}$  anti-CA125 antibody and complexed with CA125 antigen at (a) 0-, (b) 0.01-, (c) 0.1-, (d) 1-ng/ml, (e) 0.01-, (f) 0.1-, (g) 1-, (h) 10- and (i) 20- $\mu\text{g/ml}$ . The optical texture of the CA125 immunocomplex was determined by an OLYMPUS BX51 crossed polarized microscope in the transmission mode. Bar, 200  $\mu\text{m}$ .

optical texture that varied with the concentration of CA125 in a more comprehensible fashion (Fig. 6).

We determine the detection limit by comparing the LC optical textures in the presence of DI water only with those of increasing concentrations of CA125. Any gray or white spot within the area immobilized with anti-CA125 antibodies was considered to be signals produced by the CA125 immunocomplex. We thus defined the lowest CA125 concentration at which the optical texture of LCs differed from that of DI water alone as the detection limit, which was 0.01 ng/ml when an LC-based immunoassay was performed with a UV-modified DMOAP alignment layer. For immunodetection on unmodified DMOAP, the detection limit was determined as in the range of 0.01 – 0.1  $\mu\text{g/ml}$  in our previous report, in which the concentration of the anti-CA125 antibody was optimized at 0.1  $\mu\text{g/ml}$ .<sup>34</sup> The detection limit was expressed as a range of concentrations because of the relatively higher variance in optical textures when observed on unmodified DMOAP. It is, therefore, evident from our results that appropriate UV irradiation of the DMOAP alignment layer led to stronger attachment of the anti-CA125 antibodies, subsequently improving the detection limit of LC-based immunoassay.

### 3.3 Analysis of CA125-Spiked Human Serum with Liquid Crystal-Based Immunodetection

To demonstrate the potential of LC-based immunodetection in clinical application, we performed the immunoassay with CA125-spiked human serum, which was prepared by supplementing human serum with various concentrations of the CA125 antigen. The human serum contains high concentrations of proteins such as albumin and globulin as well as protein complexes that are large enough to disrupt the alignment of LCs. Because antibodies rely on noncovalent interactions such as hydrogen bonds, ionic bonds, hydrophobic interactions, and van der Waals forces to associate with antigens, these forces can also attract nonspecific proteins. Therefore, in the absence of CA125, various serum proteins and their complexes adsorb directly to UV-modified DMOAP, as well as to anti-CA125 antibodies, which bind nonspecifically to serum proteins with epitopes similar to CA125. Since no optical response was observed in the presence of anti-CA125 antibodies alone, the colorful optical texture shown in Fig. 7(a) was contributed entirely by nonspecific adsorption of the human serum. Although nonspecific binding between serum proteins and anti-CA125

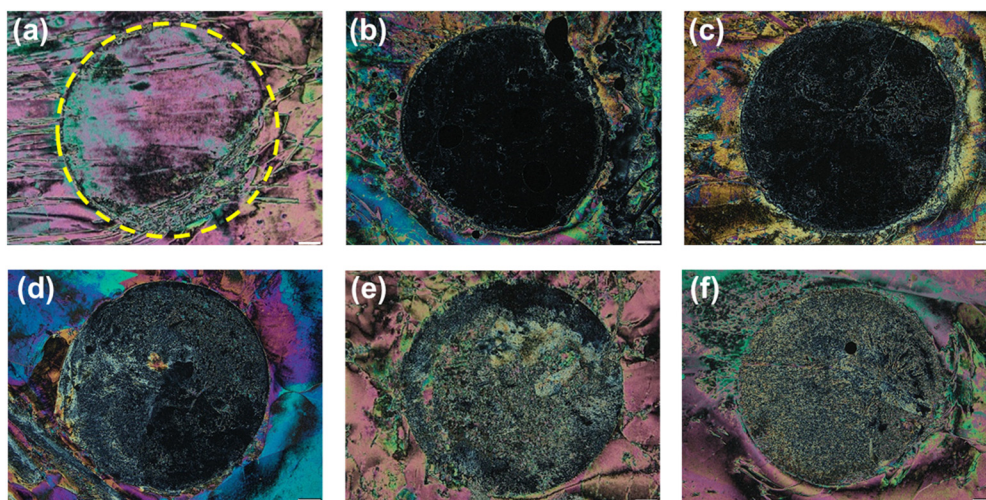


**Fig. 7** LC-based immunodetection of CA125 in CA125-spiked human serum. UV-modified DMOAP monolayer was immobilized with an array of 0.01- $\mu\text{g/ml}$  anti-CA125 antibody and reacted with CA125-spiked human serum containing (a) 0-, (b) 0.01-, (c) 0.1-, (d) 1-, (e) 10-, (f) 100-ng/ml CA125. The optical texture of the CA125 immunocomplex was determined by an OLYMPUS BX51 crossed polarized microscope in the transmission mode. Bar, 200  $\mu\text{m}$ .

antibodies was weak compared to antigen–antibody interaction, the amount of serum proteins involved in such interaction was relatively higher than in the presence of CA125 [Figs. 7(b)–7(f)]. Therefore, when the same washing procedure was applied, nonspecifically bound serum proteins cannot be efficiently removed, resulting in a high background.

The CA125 antigen exhibits stronger binding affinity toward the anti-CA125 antibody compared to nonspecific serum proteins. Thus, when the human serum was spiked with CA125, the antigen competes with serum proteins and binds specifically and preferentially to the area immobilized with the anti-CA125 antibody. Most CA125 proteins form immunocomplexes with anti-CA125 antibodies, and some adsorb directly to UV-modified DMOAP. Although serum proteins may still bind nonspecifically to anti-CA125 antibodies, the ratio is significantly reduced compared to that in Fig. 7(a) due to competition with CA125. The nonspecific and weakly bound serum proteins were subsequently removed during washing, but can still be adsorbed to the area on UV-modified DMOAP without immobilized anti-CA125 antibodies, resulting in the colorful background in Figs. 7(b)–7(f).

Meanwhile, formation of the CA125 immunocomplex gave rise to a remarkably different optical texture, which changed from dark to bright in a CA125 concentration-dependent manner [Figs. 7(b)–7(f)]. At relatively low CA125 concentrations, the amount of CA125 immunocomplexes formed may not be sufficient to create a significant disruption of LC alignment, thus the optical appearance was mainly dark. But as the concentration of CA125 was increased, gray shades in the dark area appeared, suggesting that more and more CA125 immunocomplexes were produced, and the alignment of LCs was further disrupted from the homeotropic state. These results indicate that although there were various biomolecules in the human serum with molecular weight or concentration large enough to alter the alignment of LCs, the CA125 immunocomplex formed by specific binding between the CA125 antigen and the anti-CA125 antibody resulted in a distinct optical response that enables us to distinguish specific binding from background

noise. Notably, the change in optical textures of LCs with CA125 concentration (0.01 – 100 ng/ml) in Figs. 7(b)–7(f) was consistent with that in Figs. 6(b)–6(f), demonstrating the reproducibility of the optical response in the presence of human serum. It is, thus, evident that the response obtained from LC-based immunodetection is specific and dependent on the analyte concentration, even when a complex sample of human serum was analyzed.

### 3.4 Specificity of Liquid Crystal-Based Immunodetection on Ultraviolet-Modified DMOAP

To examine the specificity of LC-based immunodetection, CA125 was reacted with the nonspecific anti-SSAT or anti- $\beta$ -catenin antibodies immobilized on UV-modified DMOAP alignment layer at 0.01  $\mu\text{g/ml}$  and 1  $\mu\text{l}$  per spot. As shown in Fig. 8, the optical textures of LCs in the presence of 0.1 or 1  $\mu\text{g/ml}$  CA125 were almost the same as the control, in which an array of anti-SSAT or anti- $\beta$ -catenin antibodies was reacted with DI water. These results indicate that immunocomplexes between CA125 and nonspecific anti-SSAT or anti- $\beta$ -catenin antibodies cannot be formed. The CA125 proteins were removed during washing or adsorbed nonspecifically to the surface of UV-modified DMOAP. Because the immobilized antibody or nonspecifically adsorbed CA125 alone was not sufficient to disturb the alignment of LCs, the orientation of LC molecules remained homeotropic, resulting in the dark optical texture.

## 4 Discussion

### 4.1 Effect of Ultraviolet Exposure on the Surface Characteristics of the DMOAP Monolayer

Although covalent linkage may enhance and stabilize the binding between the antibody and the glass surface, it requires reaction with cross-linking reagents such as glutaraldehyde or EDC/NHS, which may lead to modification of the antigen-binding

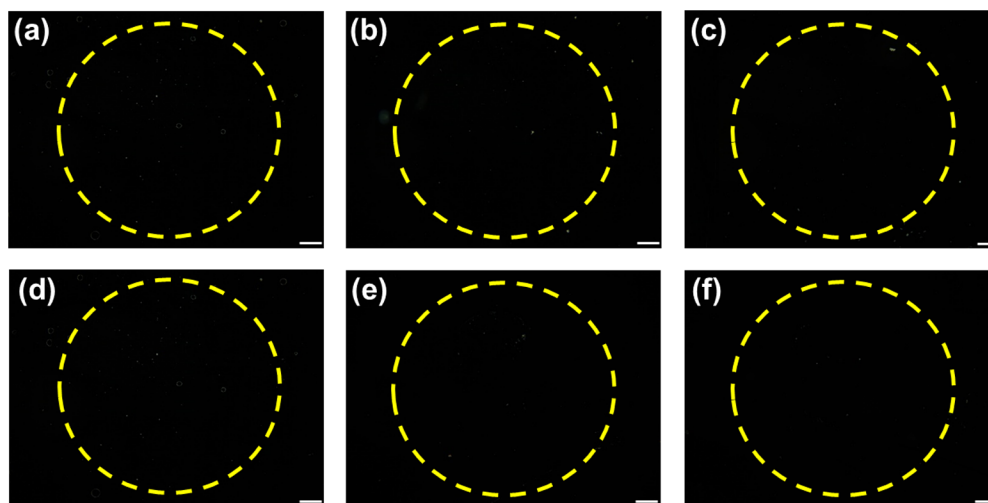


**Fig. 8** LC optical textures of CA125 reacted with nonspecific antibodies immobilized on UV-modified DMOAP alignment layer. Anti-SSAT antibodies (a–c) and anti- $\beta$ -catenin antibodies (d–f) were immobilized on UV-modified DMOAP at 0.01  $\mu\text{g}/\text{ml}$  and 1  $\mu\text{l}$  per spot, followed by reaction with (a, d) 0, (b, e) 0.1, or (c, f) 1  $\mu\text{g}/\text{ml}$  CA125 protein. Bar, 200  $\mu\text{m}$ .

site, or the paratope, of the immobilized antibody, thus reducing the binding affinity of the antibody toward the antigen. It is, therefore, preferred in this study to enhance the adsorption of the antibody by UV modification of DMOAP, so that the native structure of the antibody is not altered. Besides, the procedure for UV irradiation is relatively simple, without the need to remove residual chemicals as in the case of cross-linking reactions.

This study demonstrated that exposure to UV increased the hydrophilicity and oxygen functional groups on the DMOAP alignment layer (Figs. 3 and 4). A short exposure of DMOAP to UV (1 min) was sufficient to increase the binding efficiency of the anti-CA125 antibody without significantly altering surface hydrophilicity, and the detection limit of the LC-based immunoassay was significantly lowered compared to that utilizing unmodified DMOAP as the alignment layer (Figs. 5 and 6). Further reduction in the detection limit was not observed with prolonged UV exposure, and adverse effects such as increased background signal may possibly occur due to the degradation and loss of alignment capability of DMOAP (data not shown).

UV irradiation induces the ozonolysis reaction in which atmospheric oxygen molecules are excited, generating ozone molecules and oxygen atoms in singlet and triplet states. The oxygen atom in the singlet state exhibits strong oxidative reactivity, such that the terminal methyl groups ( $-\text{CH}_3$ ) on a self-assembled monolayer are oxidized to generate functional groups containing oxygen.<sup>38</sup> Because crosslinking reagents were not applied in this study, it is believed that the enhanced binding between UV-modified DMOAP and anti-CA125 antibodies was not contributed by covalent bonds, but possibly by increased hydrogen bonds between the oxygen functional groups of DMOAP and the polar functional groups such as  $-\text{COOH}$  and  $-\text{NH}_2$  of biomolecules.

#### 4.2 Optimal Concentration of the Anti-CA125 Antibody

As indicated in our previous study, selecting an optimal concentration of anti-CA125 antibody for immobilization is critical in

LC-based immunodetection to ensure that the immobilized antibody alone barely altered the alignment of LCs to reduce background noise, but was sufficient to interact with a wide concentration range of the CA125 antigen and produces optical responses with dose dependence.<sup>34</sup> The optimized concentration for the capture CA125 antibody is 2  $\mu\text{g}/\text{ml}$  in a dual-optical-and-electrochemical immunoassay for CA125.<sup>9</sup> In our previous study on LC-based immunodetection using intact DMOAP as the alignment layer, the optimal concentration of immobilized anti-CA125 antibodies was 0.1  $\mu\text{g}/\text{ml}$ , at which the optical response of LCs was discernible and was dependent on the concentration of the CA125 antigen.<sup>34</sup> In this study, because of the higher binding affinity provided by UV-modified DMOAP, the optimal concentration for the anti-CA125 antibody was reduced to 0.01  $\mu\text{g}/\text{ml}$ , which was applied in both immunoassays with unmodified and UV-modified DMOAP as the alignment layer for comparison (Figs. 5 and 6). Immunodetection with unmodified DMOAP was, therefore, compromised when 0.01  $\mu\text{g}/\text{ml}$  anti-CA125 antibodies were immobilized (Fig. 5). Conversely, immobilizing anti-CA125 antibodies at concentrations higher than 0.01  $\mu\text{g}/\text{ml}$  on UV-modified DMOAP generated weak background signals, which may interfere with the detection of CA125, leading to false-positive results (data not shown).

#### 4.3 Specificity of Liquid Crystal-Based Immunodetection

The specificity of LC-based immunodetection was demonstrated in our previous publications with unmodified DMOAP as well as in this study with UV-modified DMOAP (Fig. 8) using two other antibodies.<sup>34,44</sup> In the presence of nonspecific antibodies, an immunocomplex cannot be formed with CA125 to disrupt the alignment of LCs, and the optical appearance of LCs remained dark, similar to that when anti-CA125 antibodies were reacted with DI water in the absence of the CA125 antigen.

On the other hand, it is possible that CA125 itself may give rise to a nonspecific optical response at high concentrations. However, because CA125 was reacted with the entire

DMOAP-coated surface immobilized with the antibody array, nonspecific adsorption that accumulates to a detectable level can be observed in the background between spots of anti-CA125 antibodies, such as the slight perturbation in the background of Figs. 6(g)–6(i) at 1, 10, and 20  $\mu\text{g/ml}$  CA125. The dark background in Figs. 6(b)–6(f) suggests that nonspecific adsorption was mostly removed by washing, and even if there is a trace amount of CA125 adsorbed to DMOAP without interacting with the anti-CA125 antibody, the alignment of LCs was not perturbed. Consequently, because the background noise caused by the anti-CA125 antibody can be excluded by optimizing its concentration, and nonspecific adsorption of CA125 occurs only at high concentration and can be distinguished, we have eliminated the blocking procedure, which is applied in most immunoassays to avoid nonspecific binding, in our study design.

Our observations support the assumption that the larger size and molecular weight of the CA125 immunocomplex induces a more significant change in the optical texture of LC than unbound antigens or antibodies, indicating that LC-based immunodetection is capable of discerning the specific binding between antigens and antibodies from their unbound states. One can, therefore, attribute the dark-to-bright transformation of the LC optical texture to the formation of the CA125 immunocomplex. To demonstrate the feasibility of applying LC-based immunodetection in the analysis of clinical samples, we performed a proof-of-concept experiment, in which CA125-spiked human serum was reacted with the immobilized anti-CA125 antibody (Fig. 7). Although there are various biomolecules in the human serum that associate nonspecifically to UV-modified DMOAP when the blocking procedure was eliminated, resulting in a high background, the area immobilized with the anti-CA125 antibody exhibited a significantly different optical texture when CA125 was present, and a concentration-dependent response was observed. It is thus possible to simplify the procedure of LC-based immunodetection without sacrificing detection limit or specificity by directly reacting the analyte with immobilized antibody and excluding the use of blocking reagents. Moreover, identification of CA125 in human serum by LC-based immunodetection proves that it is potentially feasible to screen for cancer biomarkers in the more complex clinical sample using the method reported in this study.

## 5 Conclusions

In this study, UV-modified DMOAP alignment layers were exploited to establish a label-free and LC-based immunoassay with improved detection limit for the cancer biomarker CA125. A simple UV modification method was proposed to increase oxygen functional groups on the DMOAP alignment layer, thus enhancing binding affinity and efficiency toward anti-CA125 antibodies. In comparison with an unmodified counterpart, immunodetection on UV-modified DMOAP alignment layers exhibited a considerably lower detection limit and more significant change in LC optical texture in the presence of the CA125 antigen. In a proof-of-concept demonstration using CA125-spiked human serum as the analyte, formation of CA125 antigen–antibody immunocomplex created a distinct and concentration-dependent optical response, despite the high background resulted from the nonspecific binding of other biomolecules in human serum. Our results suggest that LC-based immunoassay holds great promise for the development of

cancer-screening technologies, and has the potential to replace conventional immunoassays.

## Acknowledgments

This study was financially supported by the Ministry of Science and Technology of Taiwan under Grant Nos. 101-2112-M-009-018-MY3 and 101-2314-B-309-001-MY3.

## References

1. H. Chen et al., "Protein chips and nanomaterials for application in tumor marker immunoassays," *Biosens. Bioelectron.* **24**, 3399–3411 (2009).
2. J. Wu et al., "Biomedical and clinical applications of immunoassays and immunosensors for tumor markers," *Trends Anal. Chem.* **26**, 679–688 (2007).
3. R. C. Bast, Jr. et al., "Reactivity of a monoclonal antibody with human ovarian carcinoma," *J. Clin. Invest.* **68**, 1331–1337 (1981).
4. L. F. Norum, B. Erikstein, and K. Nustad, "Elevated CA125 in breast cancer—a sign of advanced disease," *Tumour Biol.* **22**, 223–228 (2001).
5. M. Yamamoto et al., "Peritoneal lavage CEA/CA125 is a prognostic factor for gastric cancer patients," *J. Cancer Res. Clin. Oncol.* **133**, 471–476 (2007).
6. J. Das and S. O. Kelley, "Protein detection using arrayed microsensor chips: tuning sensor footprint to achieve ultrasensitive readout of CA-125 in serum and whole blood," *Anal. Chem.* **83**, 1167–1172 (2011).
7. N. Scholler et al., "Bead-based ELISA for validation of ovarian cancer early detection markers," *Clin. Cancer Res.* **12**, 2117–2124 (2006).
8. D. Sok et al., "Novel fluoroimmunoassay for ovarian cancer biomarker CA-125," *Anal. Bioanal. Chem.* **393**, 1521–1523 (2009).
9. I. Al-Ogaidi et al., "Dual detection of cancer biomarker CA125 using absorbance and electrochemical methods," *Analyst* **138**, 5647–5653 (2013).
10. A. Guo et al., "An ultrasensitive enzyme-free electrochemical immunosensor for CA125 using Au@Pd core-shell nanoparticles as labels and platforms for signal amplification," *J. Mater. Chem. B* **1**, 4052–4058 (2013).
11. J. Lin and H. Ju, "Electrochemical and chemiluminescent immunosensors for tumor markers," *Biosens. Bioelectron.* **20**, 1461–1470 (2005).
12. D. Tang, R. Yuan, and Y. Chai, "Electrochemical immuno-bioanalysis for carcinoma antigen 125 based on thionine and gold nanoparticles-modified carbon paste interface," *Anal. Chim. Acta* **564**, 158–165 (2006).
13. Y. Yin et al., "Colorimetric immunoassay for detection of tumor markers," *Int. J. Mol. Sci.* **11**, 5077–5094 (2010).
14. J. M. Brake et al., "Biomolecular interactions at phospholipid-decorated surfaces of liquid crystals," *Science* **302**, 2094–2097 (2003).
15. B. H. Clare and N. L. Abbott, "Orientations of nematic liquid crystals on surfaces presenting controlled densities of peptides: amplification of protein-peptide binding events," *Langmuir* **21**, 6451–6461 (2005).
16. V. K. Gupta et al., "Optical amplification of ligand-receptor binding using liquid crystals," *Science* **279**, 2077–2080 (1998).
17. Y. Y. Luk et al., "Imaging the binding ability of proteins immobilized on surfaces with different orientations by using liquid crystals," *J. Am. Chem. Soc.* **126**, 9024–9032 (2004).
18. M. L. Tingey et al., "Imaging of affinity microcontact printed proteins by using liquid crystals," *Langmuir* **20**, 6818–6826 (2004).
19. S. J. Woltman, G. D. Jay, and G. P. Crawford, "Liquid-crystal materials find a new order in biomedical applications," *Nat. Mater.* **6**, 929–938 (2007).
20. C. Y. Xue and K. L. Yang, "Dark-to-bright optical responses of liquid crystals supported on solid surfaces decorated with proteins," *Langmuir* **24**, 563–567 (2008).
21. D. Hartono et al., "Decorating liquid crystal surfaces with proteins for real-time detection of specific protein–protein binding," *Adv. Funct. Mater.* **19**, 3574–3579 (2009).
22. S. R. Kim and N. L. Abbott, "Rubbed films of functionalized bovine serum albumin as substrates for the imaging of protein–receptor interactions using liquid crystals," *Adv. Mater.* **13**, 1445–1449 (2001).
23. Y. Y. Luk et al., "Using liquid crystals to amplify protein–receptor interactions: design of surfaces with nanometer-scale topography that

- present histidine-tagged protein receptors," *Langmuir* **19**, 1671–1680 (2003).
24. X. Bi, S.-L. Lai, and K.-L. Yang, "Liquid crystal multiplexed protease assays reporting enzymatic activities as optical bar charts," *Anal. Chem.* **81**, 5503–5509 (2009).
  25. J. Hoogboom et al., "LCD-based detection of enzymatic action," *Chem. Commun.* 434–435 (2006).
  26. C.-H. Chen and K.-L. Yang, "Liquid crystal-based immunoassays for detecting hepatitis B antibody," *Anal. Biochem.* **421**, 321–323 (2012).
  27. S. R. Kim, R. R. Shah, and N. L. Abbott, "Orientations of liquid crystals on mechanically rubbed films of bovine serum albumin: a possible substrate for biomolecular assays based on liquid crystals," *Anal. Chem.* **72**, 4646–4653 (2000).
  28. Y. Y. Luk et al., "Influence of lyotropic liquid crystals on the ability of antibodies to bind to surface-immobilized antigens," *Chem. Mater.* **17**, 4774–4782 (2005).
  29. C.-Y. Xue, S. A. Khan, and K.-L. Yang, "Exploring optical properties of liquid crystals for developing label-free and high-throughput microfluidic immunoassays," *Adv. Mater.* **21**, 198–202 (2009).
  30. M. Khan and S. Y. Park, "Liquid crystal-based proton sensitive glucose biosensor," *Anal. Chem.* **86**, 1493–1501 (2014).
  31. S. Yang et al., "Gold nanoparticle based signal enhancement liquid crystal biosensors for DNA hybridization assays," *Chem. Commun.* **48**, 2861–2863 (2012).
  32. H. Tan et al., "Signal-enhanced liquid-crystal DNA biosensors based on enzymatic metal deposition," *Angew. Chem. Int. Ed.* **49**, 8608–8611 (2010).
  33. H. Tan et al., "Highly-sensitive liquid crystal biosensor based on DNA dendrimers-mediated optical reorientation," *Biosens. Bioelectron.* **62**, 84–89 (2014).
  34. H.-W. Su et al., "Label-free immunodetection of the cancer biomarker CA125 using high- $\Delta n$  liquid crystals," *J. Biomed. Opt.* **19**(7), 077006 (2014).
  35. L.-H. Ong, X. Ding, and K.-L. Yang, "Mechanistic study for immobilization of cysteine-labeled oligopeptides on UV-activated surfaces," *Colloids Surf. B Biointerfaces* **122**, 166–174 (2014).
  36. C.-H. Chen and K.-L. Yang, "Improving protein transfer efficiency and selectivity in affinity contact printing by using UV-modified surfaces," *Langmuir* **27**, 5427–5432 (2011).
  37. S. Herrwerth et al., "Factors that determine the protein resistance of oligoether self-assembled monolayers: internal hydrophilicity, terminal hydrophilicity, and lateral packing density," *J. Am. Chem. Soc.* **125**, 9359–9366 (2003).
  38. Y.-J. Kim et al., "Surface chemical conversion of organosilane self-assembled monolayers with active oxygen species generated by vacuum ultraviolet irradiation of atmospheric oxygen molecules," *Jpn. J. Appl. Phys.* **47**, 307–312 (2008).
  39. A. E. Moser and C. J. Eckhardt, "A method for reliable measurement of relative frictional properties of different self-assembled monolayers using frictional force microscopy," *Thin Solid Films* **382**, 202–213 (2001).
  40. T. Ye et al., "Photoreactivity of alkylsiloxane self-assembled monolayers on silicon oxide surfaces," *Langmuir* **17**, 4497–4500 (2001).
  41. R. G. Chapman et al., "Surveying for surfaces that resist the adsorption of proteins," *J. Am. Chem. Soc.* **122**, 8303–8304 (2000).
  42. L. Hong et al., "Photoreactivity of alkylsilane self-assembled monolayers on silicon surfaces and its application to preparing micropatterned ternary monolayers," *Langmuir* **19**, 1966–1969 (2003).
  43. J. Zheng et al., "Molecular simulation study of water interactions with oligo (ethylene glycol)-terminated alkanethiol self-assembled monolayers," *Langmuir* **20**, 8931–8938 (2004).
  44. S.-H. Sun et al., "Mesogen of large birefringence enhances the sensitivity of liquid-crystal-based immunoassays for the cancer biomarker CA125," *Biomed. Opt. Express* **6**(1), 245–256 (2015).
  45. E. A. Vogler, "Protein adsorption in three dimensions," *Biomaterials* **33**, 1201–1237 (2012).

**Hui-Wen Su** received her BS degree in biomedical engineering from I-Shou University, Kaohsiung, Taiwan, in 2012 and her MS degree in imaging and biomedical photonics from the College of Photonics, National Chiao Tung University, Tainan, Taiwan, in 2014. Her focus of research has been on liquid-crystal-based immunodetection for cancer biomarkers.

**Mon-Juan Lee** received her MS degree in chemical engineering in 2000 and her PhD in life science in 2006 from National Tsing Hua University, Hsinchu, Taiwan. Currently, she is an associate professor of the Department of Bioscience Technology with joint affiliation in the Graduate Institute of Medical Sciences at Chang Jung Christian University, Tainan, Taiwan. Her research interests include stem cell and bone biology, nanobiotechnology, as well as LC-based biomedical applications.

**Wei Lee** received his MS degree in electro-optical engineering from National Chiao Tung University (NCTU), Taiwan, in 1987 and his PhD in physics from the University of Alabama at Birmingham, Alabama, in 1993. Currently, he is the director of the Institute of Imaging and Biomedical Photonics, College of Photonics, NCTU, and the President of Taiwan Liquid Crystal Society. His primary research interests focus on liquid crystal (LC) optics and photonics including LC immunoassay applications.